the FEBS Journal

Antifungal effects and mechanism of action of viscotoxin A_3

Marcela Giudici[1,2], José Antonio Poveda[1], María Luisa Molina[1], Laura de la Canal[2], José M. González-Ros[1], Karola Pfüller[3], Uwe Pfüller[3] and José Villalaín[1]

1 Instituto de Biología Molecular y Celular, Universidad 'Miguel Hernández', Alicante, Spain
2 Instituto de Investigaciones Biológicas, Universidad Nacional de Mar del Plata, Argentina
3 Institut für Phytochemie, Private Universität Witten/Herdecke GmbH, Witten, Germany

Keywords
antifungal; cytotoxicity; defence mechanisms; mistletoe; viscotoxins

Correspondence
J. Villalaín, Instituto de Biología Molecular y Celular, Universidad 'Miguel Hernández', E-03202 Elche-Alicante, Spain
Fax: +34 966658 758
Tel: +34 966658 759
E-mail: jvillalain@umh.es

(Received 1 September 2005, revised 22 October 2005, accepted 31 October 2005)

doi:10.1111/j.1742-4658.2005.05042.x

Viscotoxins are cationic proteins, isolated from different mistletoe species, that belong to the group of thionins, a group of basic cysteine-rich peptides of ≈ 5 kDa. They have been shown to be cytotoxic to different types of cell, including animal, bacterial and fungal. The aim of this study was to obtain information on the cell targets and the mechanism of action of viscotoxin isoform A_3 (VtA_3). We describe a detailed study of viscotoxin interaction with fungal-derived model membranes, its location inside spores of *Fusarium solani*, as well as their induced spore death. We show that VtA_3 induces the appearance of ion-channel-like activity, the generation of H_2O_2, and an increase in cytoplasmic free Ca^{2+}. Moreover, we show that Ca^{2+} is involved in VtA_3-induced spore death and increased H_2O_2 concentration. The data presented here strongly support the notion that the antifungal activity of VtA_3 is due to membrane binding and channel formation, leading to destabilization and disruption of the plasma membrane, thereby supporting a direct role for viscotoxins in the plant defence mechanism.

Thionins are basic cysteine-rich proteins found in a variety of plants. They have been classified into five types according to their amino-acid sequence homology [1]. They consist of a polypeptide chain of 45–50 amino acids with three to four internal disulfide bonds, have similar 3D structures, and present a high degree of sequence homology including similarity of the distribution of hydrophobic and hydrophilic residues [2]. Thionins have different toxic activity to fungi, bacteria, animal and plant cells, which may reflect a role in plant defence, although their exact biological function is unknown [1,2]. It is supposed that their toxicity is exerted through either membrane destabilization and disruption or by channel formation or both, but their mechanism of action is not yet understood [3].

Viscotoxins are small proteins of ≈ 5 kDa isolated from leaves, stems and seeds of European mistletoe (*Viscum album* Loranthaceae). They belong to the thionin family type III and are characterized by the presence of three disulfide bridges [4,5]. The homology of viscotoxins to other thionins is restricted to the six cysteines in conserved positions (although there are also variants known from cDNAs that contain eight cysteines [6]) as well as an aromatic residue at position 13 and an arginine at position 10. To date, seven variants, A_1, A_2, A_3, B, C1, 1-PS and U-PS, have been described [5,7,8]; viscotoxin A_3 (VtA_3, Fig. 1A) is the most cytotoxic, whereas viscotoxin B (VtB) is the least potent [9,10]. The overall shape of viscotoxins is very similar to that found for the other members of the thionin family, and is represented by the Greek capital letter gamma (Γ), with two antiparallel α-helices and a short antiparallel β-sheet [7,11]. The disulfide pattern of viscotoxins is suggested to be able to stabilize a

Abbreviations
DPH, 1,6-diphenylhexa-1,3,5-triene; ROS, reactive oxygen species; SM, egg sphingomyelin; TMA-DPH, 1-(4-trimethylammoniophenyl)-6-phenylhexa-1,3,5-triene; VtA_3, viscotoxin isoform A_3; VtB, viscotoxin isoform B.

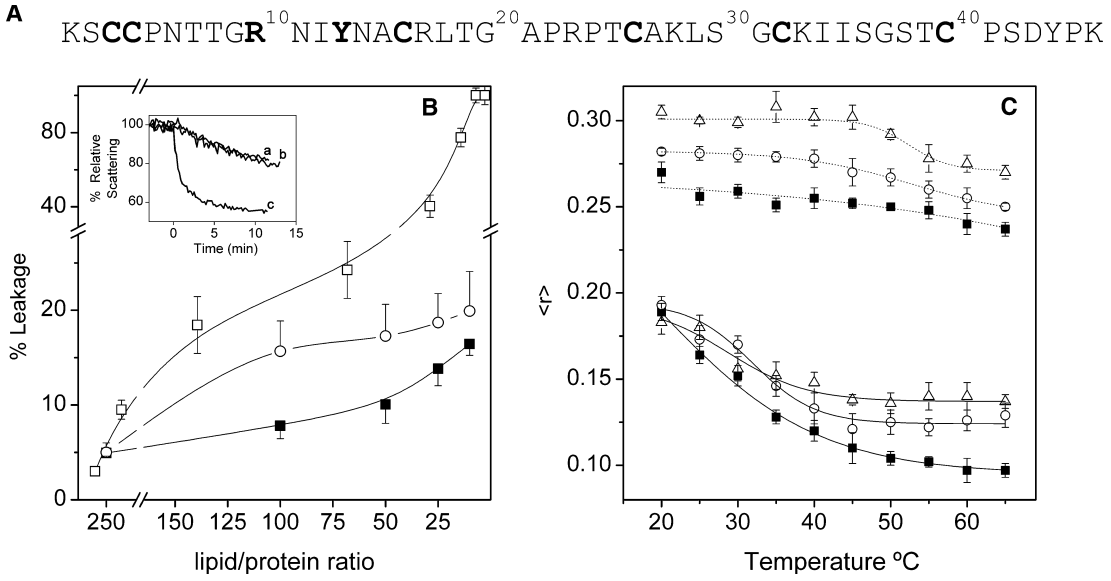

Fig. 1. (A) Sequence of VtA_3 with the conserved positions in the thionin family indicated in bold. (B) CF leakage data at 25 °C for large unilamellar vesicles composed of (■) PtdEtn/PtdSer/SM/PtdCho at molar proportions of 70 : 11 : 15 : 4, (○) PtdCho/PtdEtn/PtdSer at molar proportions of 45 : 45 : 10, and (□) lipids extracted from fungal spores in the presence of VtA_3 at different lipid/protein ratios. (C) Steady-state anisotropy, $<r>$, of (—) DPH and (····) TMA-DPH incorporated into spores of *F. solani* in the absence of VtA_3 (■) and in the presence of 1.5 μM VtA_3 (○) and 3 μM VtA_3 (△). Insert in (B) shows the evolution of the scattering peak (membrane disruption) for (a) lipids extracted from fungal spores, (b) PtdCho/PtdEtn/PtdSer at molar proportions of 45 : 45 : 10 and (c) PtdEtn/PtdSer/SM/PtdCho at a molar proportions of 70 : 11 : 15 : 4 after addition of VtA_3 to give a lipid/protein ratio of 10 : 1.

common structure occurring in various small proteins able to interact with cell membranes [3,5,12]. In spite of many reports on viscotoxins, their biological role is still unclear. They have been considered to be storage proteins as well as linked to plant defence as its high expression gives enhanced resistance to pathogens [13]. Viscotoxins display different toxic activities towards a number of tumour cell lines, suggesting that the different observed cytotoxicity could reflect variations in secondary structure and/or types of interaction [5,9,10,14,15]. We have previously reported on the antifungal activity of VtA_3 and VtB towards three phytopathogenic fungi (*Fusarium solani*, *Sclerotinia sclerotiorum* and *Phytophtora infestans*), showing minimum inhibitory concentrations of the order of 1.5–3.75 μM [16]. We have also reported the interaction of VtA_3 and VtB with model membranes and suggested that their biological activity may be ascribed to membrane permeabilization [3]. It has also been found that viscotoxins increase cell-mediated killing of tumour cells, exert a strong immunomodulatory effect on human granulocytes, alter membrane permeability, generate ROS (reactive oxygen species), produce cell death in human lymphocytes, and induce the generation of H_2O_2 in spores [9,15–18].

In this work we have gained more information on the cellular targets and the mechanism of action of viscotoxins, by examining the interaction of VtA_3 with fungal cells. We describe a detailed investigation of the cellular and signalling characteristics of VtA_3-induced spore death in *F. solani*, its effect on fungal-derived membranes, its location inside *F. solani* spores, as well as its pore-forming ability. Our results strongly support the notion that the antifungal activity of VtA_3 is due to membrane binding and subsequent pore formation, destabilization and disruption of the membrane, leading to cell death.

Results

We have previously reported the interaction of both VtA_3 and VtB with phospholipid model membranes as well as the ability of VtA_3 to modify the permeability of fungal membranes, suggesting that its biological activity may be ascribed to membrane permeabilization [3,16]. To further explore the interaction of the most cytotoxic viscotoxin isoform, VtA_3, with biological membranes and obtain information on its mechanism of action, we have applied different techniques as shown below. The exact composition of the lipid membranes of *F. solani* has not previously been reported, but using TLC we observed that the major lipids are PtdCho, PtdEtn and PtdSer in the approximate molar proportions 45 : 45 : 10. Here we studied the effects of

VtA_3 on liposomes, both constituted from the natural lipids extracted from spores of *F. solani* and artificial liposomes resembling either general fungal spore plasma membranes or *F. solani*-specific plasma membranes [33,34], i.e. liposomes composed of PtdEtn/PtdSer/SM/PtdCho (SM, sphingomyelin) and PtdCho/PtdEtn/PtdSer at molar proportions 70 : 11 : 15 : 4 and 45 : 45 : 10, respectively (Fig. 1B). Leakage was found to depend on lipid composition, as the extent of leakage from liposomes composed of lipids extracted from *F. solani* spores is greater than in fungi-like liposomes. It is interesting to note that, for liposomes composed of spore lipids, an approximate concentration of 10 μM VtA_3 induced 100% leakage (≈ 65% for VtB, results not shown). Significantly, a decrease in scattering (increase in membrane rupture) was also observed on addition of VtA_3 (insert Fig. 1B). The increase in leakage and decrease in scattering elicited by VtA_3 demonstrate the capacity of the protein to destabilize and disrupt membranes at low lipid/protein ratios.

We also studied the dynamics of the *F. solani* spore membrane lipids in the presence of VtA_3 by measuring fluorescence anisotropy of 1,6-diphenylhexa-1,3,5-triene (DPH) and TMA-DPH [1-(4-trimethylammoniophenyl)-6-phenylhexa-1,3,5-triene] inserted in living spore suspensions (Fig. 1C). The diphenylhexatrienyl moiety of DPH is distributed about a central position in the bilayer (inner probe), whereas its charged derivative, TMA-DPH, extends into the lipid bilayer between the C5 and C11 carbons of the phospholipid acyl chains (interfacial probe), reporting essentially structural information on this region of the bilayer [35]. As observed in Fig. 1C, both DPH and TMA-DPH fluorescence anisotropies increased at increasing concentrations of VtA_3, indicating that VtA_3 interacts with fungal membranes, increasing its rigidity at all temperatures. These results provide evidence that VtA_3 is incorporated into the spore membrane as well as modulating its biophysical properties.

The next experiments were designed to analyze whether VtA_3 was able to enter intact *F. solani* cells. VtA_3 was labelled with Texas Red and monitored by confocal microscopy (see Experimental procedures). The antifungal activity of Texas Red-labelled VtA_3 was previously shown to have the same toxicity as wild-type VtA_3, as 10 μM Texas Red-labelled VtA_3 completely abolished the germination of *F. solani* spores (results not shown). As observed in Fig. 2A, the protein seemed to accumulate inside the cells, demonstrating for the first time that VtA_3 can enter and accumulate inside fungal cells. In addition we analyzed whether Texas Red-labelled VtA_3, like the unlabelled form, was capable of modifying the permeability of fungal membranes [16]. We used the fluorescent probe Sytox® Green, which only enters cells with a damaged membrane, binding subsequently to nucleic acid and emitting fluorescence. Figure 2B shows that fungal cells incorporated the fluorescent probe, indicating that membrane damage was produced when the cells where incubated with Texas Red-labelled VtA_3. We also examined the possibility that Texas Red-labelled VtA_3 could enter giant liposomes, composed of PtdCho/PtdEtn/PtdSer at molar proportions 50 : 25 : 25, as the theoretical composition of *F. solani* membrane phospholipid (PtdCho/PtdEtn/PtdSer, 45 : 45 : 10) would not form stable multilamellar giant liposomes. Figure 2D shows that VtA_3 was not capable of translocating through the phospholipid bilayer of liposomes, as we could only see the protein bound to the external monolayer.

A possible explanation for the effect of VtA_3 on fungal cells could be that this protein would form ion channels or pores in cell membranes, as reported for other members of the thionin family [36,37]. We investigated this possibility by using patch-clamp methods to study the effects of VtA_3 added to the bath solution on excised, inside-out membrane patches from asolectin giant liposomes. Such liposomes have been used previously to explore the channel-forming ability of other thionins [37]. Control experiments in the absence of added VtA_3 showed no electrical activity whatsoever in the excised asolectin membrane patches (not shown). Moreover, no activity was found when VtA_3 (up to 3 μM, $n = 8$) was added to the bath solution of membrane patches held at a membrane potential of 0 mV. In contrast, when the membrane patches were subjected to the potential pulse protocol described in Experimental Procedures after VtA_3 addition, electrical activity was detected at different toxin concentrations in 85% ($n = 23$) of the patches assayed, suggesting that, under our experimental conditions, triggering of the channel formation requires a membrane potential different from zero. Indeed, the activity begins to be observed mostly when the membrane is subjected to a positive voltage, and, from there on, it continues being present at any of the voltages assayed in the pulse protocol. In the 0.1–1 μM range of added VtA_3 ($n = 12$; 44% of the active patches), we found ion-channel-like activity in the form of square pulses of current (Fig. 3A). Such activity was always preceded by an increase in the recording's baseline, suggesting that toxin incorporation induced an increase in the membrane conductance. Single-channel current vs. voltage (I/V) plots of the activity recorded at concentrations of 1 μM VtA_3 ($n = 7$) (Fig. 3C) shows a significant open-channel rectification. Also, under the

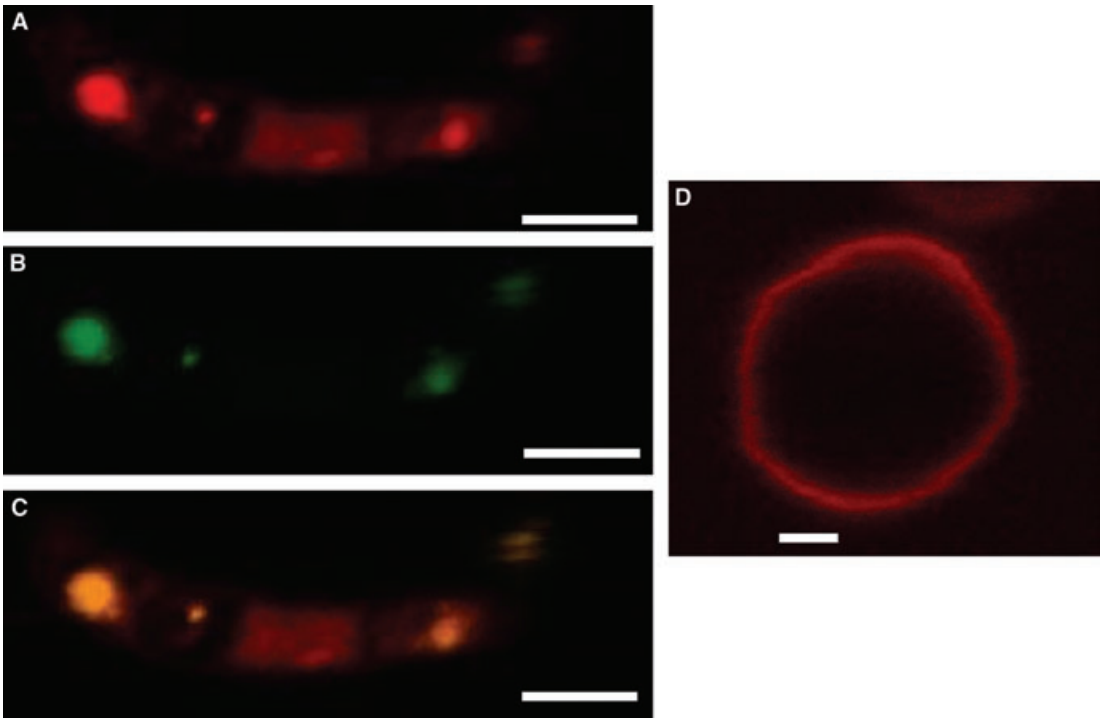

Fig. 2. Confocal laser scanning images of Texas Red-labelled VtA_3 bound to (A, B, C) *F. solani* spores and (D) giant liposomes composed of egg PtdCho/egg PtdEtn/brain PtdSer at molar proportions of 50 : 25 : 25. *F. solani* spores and giant liposomes were incubated with 10 μM Texas Red–VtA_3 for 5 min, and then viewed under a confocal laser scanning microscope. When spores were used, Sytox® Green was added just before being viewed under the microscope. Spore image is split into two fluorescence channels, 543 nm excitation for VtA_3–Texas Red (A), 488 nm excitation for Sytox® Green (B) and the overlay image of the two excitation wavelengths (C). Giant liposomes were viewed with 543 nm excitation (D). Images are representative of five different experiments. The scale bar represents 5 μm.

asymmetrical ionic conditions used in these experiments, i.e., using a KCl concentration gradient, a reversal potential value of $+27.6 \pm 6$ mV ($n = 7$) was estimated, which is quite different from the equilibrium potential for K^+ under these conditions (+ 59.2 mV). The latter observation suggests that the putative channels formed by the toxin are only moderately selective for cations, which is similar to previous reports on others member of the thionin protein family [36,37]. Interestingly, the observed channel-like gating activity was always found to be transient and, depending on the VtA_3 concentration, lasted from a few seconds up to five minutes, after which, an abrupt increase in membrane leakage occurred, indicating membrane disruption (Fig. 3A; the histogram with the distribution of current amplitudes is also shown in Fig. 3B). This disruption process was practically instantaneous ($n =$ 11, 41% of the cases) when higher concentrations (up to 3 μM) of toxin were used in the experiments. In an attempt to mimic the lipid composition of the physiological target more closely, we also tried to obtain inside-out membrane patches from giant liposomes made of PtdCho/PtdEtn/PtdSer mixtures at molar proportions 50 : 25 : 25 and 45 : 45 : 10. However, the resulting liposomes did not allow a proper high resistance seal with the patch pipette, and this possibility was discarded.

We have previously shown that spores, in the presence of VtA_3 at a concentration of 10 μM and after 8 h of treatment, produce H_2O_2 [16], suggesting that it may be an intermediate in VtA_3 cytotoxicity. This fact, together with the observed location of VtA_3 in living spores, prompted us to study the relationship between the presence of VtA_3 and H_2O_2 production. We improved the previous experiments [16] by using a highly H_2O_2-sensitive probe, Amplex Red, and correlated H_2O_2 production with spore viability as shown in Fig. 4. When VtA_3 concentration was increased, H_2O_2 production increased concomitantly (Fig. 4A). Interestingly, the insert in Fig. 4A shows that H_2O_2 production is dependent on the incubation time and the concentration of VtA_3. In a similar manner, spore death (detected as propidium iodide stain) increased in a dose-dependent way as observed in Fig. 4B. The direct correlation between spore death and H_2O_2 production is observed in the insert of Fig. 4B. We

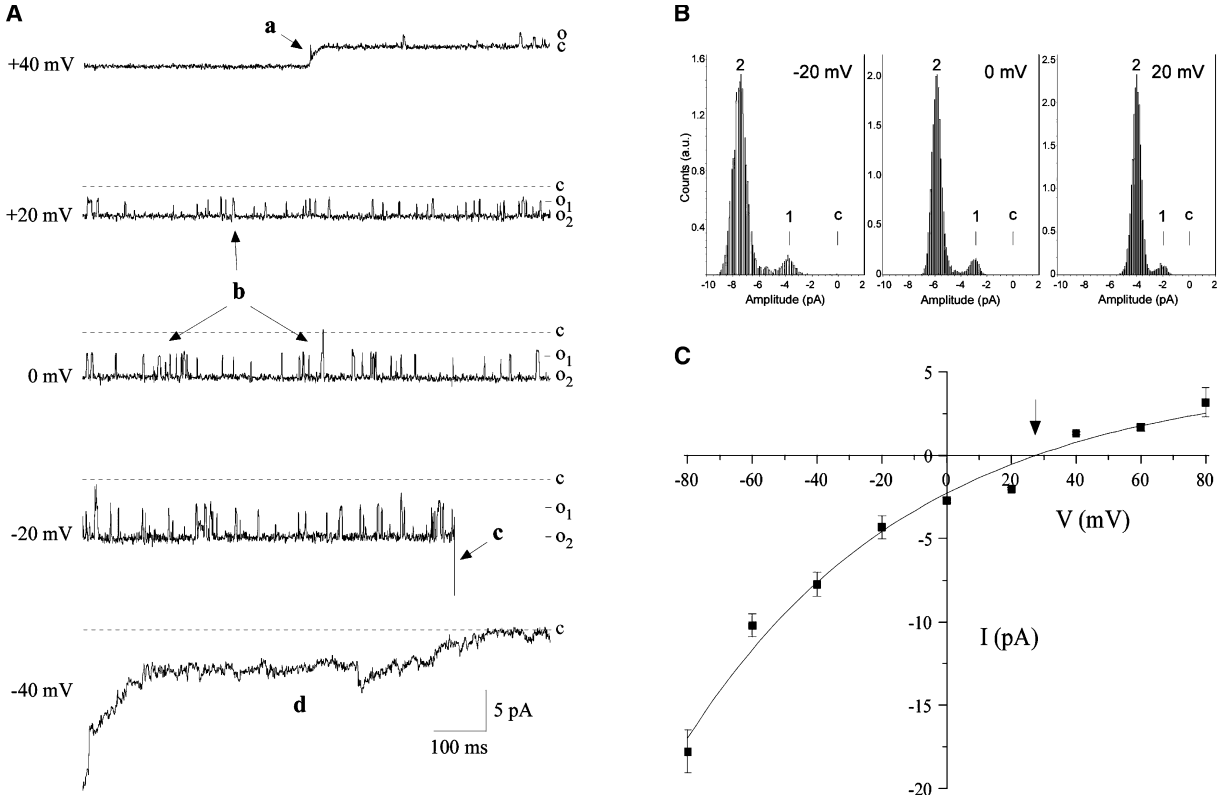

Fig. 3. (A) Representative patch clamp recordings from a series of membrane potential pulses from positive to negative voltage illustrating the effects of addition of 1 μM VtA_3 to the bath solution in excised patches from asolectin giant liposomes. The zero current level at each voltage is indicated by a dotted line. Typically, 30 s after the addition of the toxin to the bath solution, an increase in the membrane baseline conductance was observed (a), followed by the appearance of channel-like openings in the form of square currents (b), which covered one or two open-channel states of the same amplitude (O_1 and O_2). Eventually, an abrupt increase in membrane leakage took place (c), which led to membrane rupture (d) and to the disappearance of ion channel activity. (B) Amplitude histograms calculated from the single-channel trajectories for recordings shown in (A). (C) Average single-channel current vs. voltage plot of the VtA_3-induced ion-channel-like activity in the excised asolectin membranes patches. A KCl gradient (10 and 100 mM KCl in the bath and pipette solutions, respectively) was used in these experiments. Current amplitudes at each voltage were calculated by averaging the single square current amplitudes. The arrow indicates the reversal potential under these asymmetrical conditions.

observed an enhanced accumulation of Rhodamine 123 in fungal cells (not shown for briefness), indicating that VtA_3 provokes either hyperpolarization of the inner mitochondrial membrane or swelling of mitochondria or both [9,38].

Cytosolic Ca^{2+} plays a crucial role in cell signalling and can regulate a wide range of physiological functions in diverse organisms [39]. To determine if the different biological effects elicited by VtA_3 in fungal spores are related to changes in internal Ca^{2+} concentration, we measured the concentration of free cytosolic Ca^{2+} at different VtA_3 concentrations and different incubation times as shown in Fig. 5. At increasing VtA_3 concentrations and incubation times, free cytosolic Ca^{2+} increased, showing that either directly or indirectly cytosolic Ca^{2+} is indeed related to the biological effects elicited by VtA_3 (*vide supra*). With the aim of determining if the increase in free cytosolic Ca^{2+} concentration induced by the presence of VtA_3 is related to either cell viability or H_2O_2 production or both, we treated the spores with VtA_3 in the presence of the Ca^{2+} chelator Bapta-AM. The results are shown in Fig. 6. The increase in Bapta-AM concentration, i.e. decrease in free Ca^{2+} availability, abolished both H_2O_2 production and spore death induced by VtA_3 (Fig. 6A and 6B, respectively). To determine the origin of this cytosolic Ca^{2+}, we incubated the spores with the voltage-dependent Ca^{2+} channel blocker verapamil at various concentrations in the presence of 10 μM VtA_3, but no effect was observed on either spore viability or H_2O_2 production (not shown for brevity). On the other hand, depletion of Ca^{2+} caused by external EGTA in the millimolar range did not reduce H_2O_2 production by VtA_3. All these data suggest that the

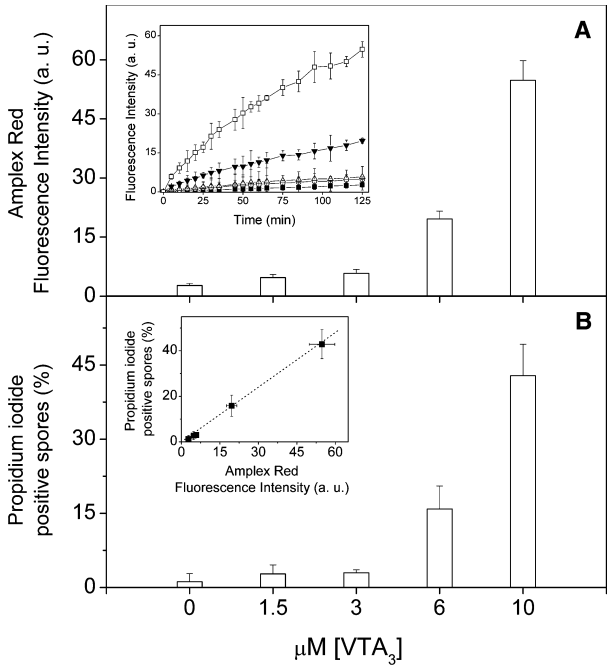

Fig. 4. Effect of VtA_3 on H_2O_2 production (A) and spore viability (B) after incubation for 2 h. Insert in (A) shows H_2O_2 production as a function of time for 0 μM (■),1.5 μM (○), 3 μM (△), 6 μM (▽) and 10 μM (□) of VtA_3, whereas the insert in (B) shows the relationship between spore viability and H_2O_2 production.

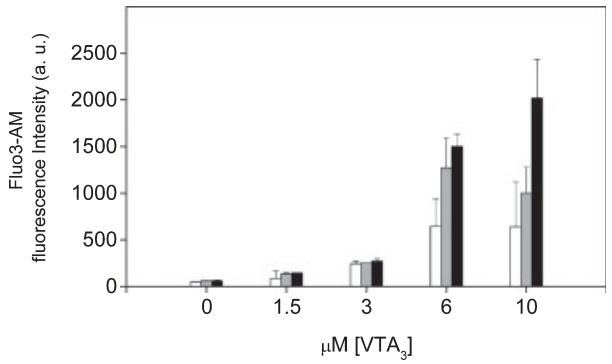

Fig. 5. Increase in intracellular free Ca^{2+} measured in *F. solani* spores incubated with different concentrations of VtA_3 for 5 min (white), 15 min (grey) and 45 min (black).

increase in Ca^{2+} concentration in the cytosol after VtA_3 incubation originates from internal Ca^{2+} stores (vacuoles, endoplasmic reticulum, etc.).

Discussion

It has been known for many years that thionins inhibit the growth of fungi *in vitro* [40]; furthermore, we have shown very recently that viscotoxins have potent antifungal activity affecting both spore germination and hyphal growth of phytopathogenic fungi, reinforcing the idea that viscotoxins would be useful compounds for controlling fungal pathogens in plants [16]. We used for the first time model membranes with a lipid composition derived from intact spores in order to observe the capability of destabilization and/or disruption of bilayer membranes by VtA_3. We show that VtA_3 had a significant effect on integrity and permeability of liposomes composed of fungal-extracted lipids. We also show the modulation of the biophysical properties of fungal membranes by VtA_3 by the increase in the fluorescence anisotropy of both inner and interfacial probes inserted in spore membranes. The change in fluidity of fungal membranes may be explained by the insertion of the protein and modulation of the lateral pressure, as has been reported for other proteins [41]. Moreover, these results confirm that VtA_3 affects the whole structure of the membrane and demonstrate that it inserts into the membrane palisade. These results are consistent with previous observations that suggested that the perturbations induced by viscotoxins were related to alteration of membrane fluidity [3].

Even though the order of events leading to cell death provoked by viscotoxins are not exactly known, membrane permeabilization should be an early effect. Indeed there is a relationship between spore viability, H_2O_2 production and VtA_3 concentration as shown in this work, which would indicate that the H_2O_2 production and subsequent cell death may be a consequence of membrane perturbation. It is interesting to note here that VtA_3 concentrations ranging from 3 to 10 μM induced membrane disruption as well as giving rise to H_2O_2 production and spore death. These concentrations are higher than those previously reported [16], as we used short incubation times (IC_{50} for VtA_3 was found to be about 1.5–3.75 μM after 48 h of incubation time).

It has been previously shown that thionins mediate transient fluxes of Ca^{2+} in *Neurospora crassa* hyphae [42]. We found that VtA_3 induced an increase in internal Ca^{2+} concentration, this Ca^{2+} probably being liberated from internal stores. We were able to detect cytoplasmic free Ca^{2+} in the presence of both VtA_3 and EGTA, and, in addition, labelled VtA_3 inside spore cells. The cytoplasmic Ca^{2+} increase elicited by VtA_3 may therefore be related to permeabilization of those organelles. Viscotoxins, apart from disturbing and rupturing membranes (*vide supra*), can induce the generation of ROS intermediates as well as apoptosis-related changes in different types of cell [9,16]. We have not detected VtA_3-induced apoptosis, although necrosis could not be ruled out. As

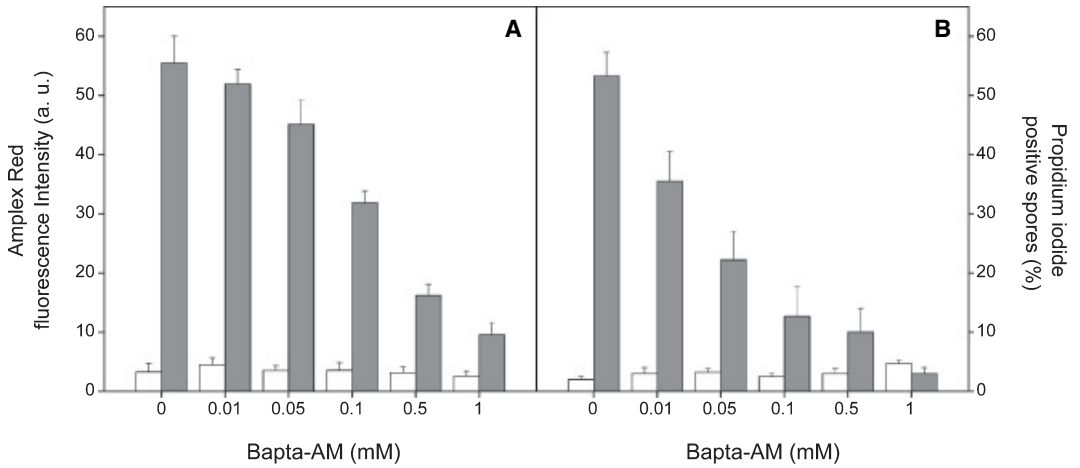

Fig. 6. Correlation between cytosolic Ca^{2+}, VtA_3, and (A) H_2O_2 production and (B) cell viability. *F. solani* spores were preincubated with different concentrations of Bapta-AM for 40 min as indicated and then incubated with 10 μM VtA_3 for 2 h (grey columns). Control untreated samples are depicted as white columns.

noted previously, the major functional impact of cell necrosis would be the loss of mitochondrial inner-membrane potential, excess of ROS intermediates, and a decrease in ATP production [43]. As mentioned above, VtA_3 induces either hyperpolarization of the inner mitochondrial membrane or mitochondrial swelling or both; cells in which mitochondria are destabilized and finally broken down suffer a decrease in the coupling efficiency of the electron-transport chain and therefore can generate ROS intermediates, which can lead to oxidative stress [43].

VtA_3 cannot span the bilayer because the two antiparallel α-helices are much shorter than the bilayer thickness, so that a single VtA_3 molecule cannot form an ion-channel-like structure. Therefore, we have to assume that individual VtA_3 molecules must somehow assemble as a transmembrane complex for ion-channel-like activity to appear. This has been shown to be the case for the channel-forming antibacterial protein sapecin [44]. Moreover, it has been reported that viscotoxins can form complexes in both solution and crystals [45,46], supporting the notion that such a complex may also be formed inside the membrane to account for the observed ion-channel-like activity [47]. Therefore, the lag time observed between the increase in membrane conductance and the appearance of channel activity may be related to the assembly of the putative complex into the bilayer. Whatever the case might be, channel formation does not preclude the existence of additional mechanisms of bilayer breakdown. In fact, we have been able to observe channel formation, but only at relatively low viscotoxin concentration as concentrations greater than 1 μM always led to seal breakdown. *Pyrularia* thionin and β-purothionin are also capable of lysing cell membranes, indicating that thionins in general have lytic capabilities [36,48]; β-purothionin is also capable of forming channels in membranes [36]. In a similar way, melittin is also highly lytic. It has been proposed to act via a two-step mechanism in killing cells [49], initially acting as an ion channel to depolarize cells and, if present at a sufficient concentration, lysing cells directly. Viscotoxins may behave in a similar way.

We also observed that incorporation of the toxin into the membrane bilayer appears to be dependent on the existence of a membrane potential established between the two sides of the bilayer. It is interesting to note that membrane permeabilization induced by plant defensins appears to require a polarized membrane [42]. It may be that, like defensins, viscotoxins require a polarized membrane for channel formation, as indicated in this work. This is consistent with previous suggestions made for other thionins [3,36,42,50], in which the electrostatic interaction of these positively charged proteins play an essential role as a first step in their interaction with membranes. It is interesting to note the absence of translocation of VtA_3 through the liposome bilayers compared with the translocation observed *in vivo* in *F. solani* spores. This difference in translocation may be related not only to differences in bilayer composition but also to the existence of a polarized membrane, as mentioned above. However, membrane disruption would not depend on the presence of a polarized membrane but on membrane composition [51,52].

It is unclear why amphipathic polypeptides such as thionins from mistletoe and other plants with close structural identity show quite different biological

behaviour. The toxicity of β-purothionin may be due to its ability to form ion channels in cell membranes [36], whereas the toxicity of α-hordothionin and wheat α-thionin originates through binding to the membrane surface and disturbance of its organization [42,50]. VtA_3 may have both properties. Viscotoxins in general may bind to membranes and form ion channels or pores at low concentrations, but at higher concentrations they may directly lyse the membrane, i.e. they would behave like a detergent [3]. Furthermore, the interaction of viscotoxins and fungal cells may also lead to other secondary effects, such as H_2O_2 production and Ca^{2+} liberation. This membranotropic effect may explain the high toxicity of viscotoxins in particular and thionins in general. In conclusion, our results strongly support the notion that the antifungal activity of VtA_3 is due to the occurrence of a number of processes, including initial membrane binding and subsequent pore formation, followed by destabilization and disruption of both plasma and inner membranes.

Experimental procedures

Reagents

Trans-esterified egg L-α-phosphatidylethanolamine (PtdEtn), egg L-α-phosphatidylcholine (PtdCho), bovine brain phosphatidylserine (PtdSer), and egg sphingomyelin (SM) were obtained from Avanti Polar Lipids (Alabaster, AL, USA). CHAPS {3-[(3-cholamidopropyl)dimethylammonio]-1-propanesulfonate}, 5-carboxyfluorescein (> 95% by HPLC), 2-(6-amino-3-imino-3*H*-xanthen-9-yl)benzoic acid methyl ester (Rhodamine 123), asolectin type II, ampicillin and horseradish peroxidase were obtained from Sigma-Aldrich (Madrid, Spain). DPH, TMA-DPH, PBFI-AM {1,3-benzenedicarboxylic acid 4,4′-[1,4,10,13-tetraoxa-7,16-diazacyclo-octadecane-7,16-diylbis(5-methoxy-6,2-benzofurandiyl)] bis-tetrakis[(acetyloxy)methyl]ester}, Fluo3-AM {1-[2-amino-5-(2,7-dichloro-6-hydroxy-3-oxo-9-xanthenyl)phenoxy]-2-(2-amino-5-methylphenoxy)ethane-*N*,*N*,*N*′,*N*′-tetra-acetic acid, pentaacetoxymethyl ester}, Bapta-AM [*O*,*O*′-bis(2-aminophenyl)ethyleneglycol-*N*,*N*,*N*′,*N*′-tetra-acetic acid, tetra-acetoxymethyl ester], Amplex Red (*N*-acetyl-3,7-dihydroxy phenoxazine), Sytox® Green, Texas Red sulfonyl chloride [1*H*,5*H*,11*H*,15*H*-xantheno(2,3,4-*ij*:5,6,7-*i*′j′)diquinolizin-18-ium,9-(2(or4)-(chlorosulfonyl)-4(or2)-sulfophenyl)-2,3,6,7,12,13,16,17- octahydro-, hydroxide] were obtained from Molecular Probes (Eugene, OR, USA). Propidium iodide was obtained from BD Biosciences (Madrid, Spain). All other reagents used were of analytical grade from Merck (Darmstad, Germany). Water was deionized, twice-distilled and passed through a Milli-Q equipment (Millipore Ibérica, Madrid, Spain) to a resistivity better than 18 MΩ cm.

Biological materials

Fusarium solani f. sp. *eumartii*, isolate 3122 (EEA-INTA, Balcarce, Argentina), was grown at 25 °C on potato dextrose agar plates supplemented with 100 $\mu g \cdot mL^{-1}$ ampicillin, and spores were collected from 8-day-old cultures by suspension in sterile water.

Protein purification

Viscotoxins were prepared and extracted as described previously [3,10]. Briefly, fresh plant material (leaves and stems) from *V. album* L. was homogenized in 2% acetic acid, diluted with distilled water, and passed through a cation-exchange column. After a washing step, the adsorbed proteins were eluted with 0.1 M HCl, neutralized with $NaHCO_3$ and fractionated by HPLC. Individual viscotoxins were finally isolated by HPLC on a C_4 reverse-phase column [3]. The proteins were dissolved in 0.1% trifluoroacetic acid, loaded on to the column equilibrated with 20% acetonitrile in 0.1% trifluoroacetic acid and eluted by linear gradient from 20% to 50% acetonitrile in 0.1% trifluoroacetic acid over 30 minutes at a flow rate of 1 $mL \cdot min^{-1}$. The protein concentration was measured as described [19].

Lipid extraction from spore cells

Lipid extraction from spore cells was performed according to the Bligh and Dyer procedure using the proportions 1 : 1 : 0.9 (v/v/v) between chloroform/methanol and the corresponding aqueous sample [20]. Polar lipids were fractionated by 1D TLC on activated 0.2-mm layers of high-performance 10 × 10 cm plates (LHP-K, Whatman Brentford, UK). Aliquots containing 70 μg total lipid were developed using chloroform/methanol/concentrated ammonia (65 : 25 : 4, v/v). Lipid spots were visualized by exposure to an iodine-saturated atmosphere. The phospholipid concentration was measured as described [21].

Assay of plasma membrane fluorescence anisotropy

Fungal cells were incubated at 25 °C in 10 mM Hepes, pH 7.4, for 30 and 60 min with either 6.6×10^{-4} mM TMA-DPH or 8.5×10^{-4} mM DPH, respectively [22]. Afterwards cells were incubated for 1 h with different concentrations of VtA_3 as stated in the figures. Fluorescence measurements were carried out using a SLM 8000C spectrofluorimeter with a 450-W Xe lamp, double-emission monochromator, and Glan-Thompson polarizers. Correction of excitation spectra was performed using a Rhodamine B solution. Typical spectral bandwidths were 4 nm for excitation and 2 nm for emission. All fluorescence studies were carried out using 5 mm × 5 mm quartz cuvettes. The

excitation and emission wavelengths were 360/425 and 362/450 nm for observation of the fluorescence of DPH and TMA-DPH, respectively. Fluorescence anisotropies were determined as described [3].

Assay for leakage of liposomal contents

Aliquots containing the appropriate amount of lipid in chloroform/methanol (2 : 1, v/v) were placed in a test tube, the solvents removed by evaporation under a stream of O_2-free nitrogen and finally traces of solvents were eliminated under vacuum in the dark for more than 3 h. Then, 1 mL buffer containing 10 mM Tris/HCl, 20 mM NaCl, pH 7.4, and 5-carboxyfluorescein at a concentration of 40 mM was added, and multilamellar vesicles were obtained. Large unilamellar vesicles with a mean diameter of 90 nm were prepared from multilamellar vesicles by the extrusion method [23] using polycarbonate filters with a pore size of 0.1 μm (Nuclepore Corp., Cambridge, CA, USA). Non-encapsulated 5-carboxyfluorescein was separated from the vesicle suspension on a Sephadex G-75 filtration column (Pharmacia, Uppsala, Sweden) eluted with buffer containing 10 mM Tris/HCl, 0.1 M NaCl and 1 mM EDTA, pH 7.4. Leakage was assayed by treating the probe-loaded liposomes (final lipid concentration 0.1 mM) with the appropriate amounts of VtA_3 in a fluorimeter cuvette stabilized at 25 °C. Changes in fluorescence intensity were recorded on a Varian Cary spectrofluorimeter interfaced with a Peltier element for temperature stabilization, with excitation and emission wavelengths set at 492 and 516 nm, respectively. Data were acquired using excitation and emission slits at 5 nm. Complete release was achieved by adding to the cuvette Triton X-100 to a final concentration of 0.1% (w/w). Leakage was quantified on a percentage basis according to the equation: % release $= [(F_f - F_0)/(F_{100} - F_0)] \times 100$. F_f is the equilibrium value of fluorescence 10 min after protein addition, F_0 the initial fluorescence of the vesicle suspension, and F_{100} the fluorescence value after addition of Triton X-100.

Light scattering measurements

The ability of VtA_3 to change large unilamellar vesicle scattering was used as an indicator of liposome integrity. Right-angle light scattering was measured using a Varian Cary spectrofluorimeter with both excitation and emission monochromators set at 400 nm [24]. Data were acquired using excitation and emission slits at 2.5 nm. Samples containing liposomes (final lipid concentration 0.1 mM) and the appropriate amount of VtA_3 were placed in a 5 mm × 5 mm fluorimeter cuvette stabilized at 25 °C under constant stirring. No scattering was achieved by adding Triton X-100 to the vesicle suspension to give a final concentration of 0.1% (w/w).

Measurement of intracellular K^+

Spores were resuspended in 10 mM Hepes, pH 7.4, and incubated with the cell-permeant form of the K^+-binding fluorescent dye benzofuran isophthalate, PBFI-AM (final concentration, 5 μM PBFI-AM) for 2 h at 25 °C, washed twice and resuspended in 10 mM Hepes, pH 7.4, to a final density of 2.2×10^7 spores·mL^{-1}. Variations in intracellular K^+ content were expressed as a fraction of PBFI-AM maximal fluorescence intensity [25]. Fluorescence measurements were carried out at 25 °C using a SLM 8000C spectrofluorimeter with a 450-W Xe lamp, double-emission monochromator, and Glan-Thompson polarizers using quartz cuvettes with continuous stirring of the suspension, bandwidths of 2 nm for excitation and 4 nm for emission, and excitation and emission wavelengths of 360 and 500 nm, respectively.

Mitochondrial transmembrane potential

Mitochondrial transmembrane potential was assayed by adding the cationic fluorochrome Rhodamine123 in 10 mM Hepes, pH 7.4, to cultured cells for 10 min at 37 °C in the dark (final concentration 50 nM) as previously described [26]. Fluorescence was detected with a Leica inverted microscope with a digital camera.

Viability assay

Spores were incubated for 10 min with 100 μg·mL^{-1} propidium iodide in buffer containing 10 mM Hepes/NaOH, 140 mM NaCl, and 2.5 mM $CaCl_2$, pH 7.4, as described previously [27]. Spores were quantified using a Neubauer camera in a Fluorescent microscopy Leica DMIRB, acquisition camera Leica DC 250 and Qfluoro V 1.2.0 software.

Detection of H_2O_2

H_2O_2 was determined enzymatically as described [27]; samples contained 2×10^7 spores·mL^{-1}, 1 U·mL^{-1} horseradish peroxidase and 7.5 μM Amplex Red in 10 mM Hepes, pH 7.4, buffer. Fluorescence measurements were performed using a Varian Cary spectrofluorimeter interfaced with a Peltier element for temperature stabilization. The emission and excitation slits were 5 nm.

Cytosolic Ca^{2+} measurements

Cytosolic Ca^{2+} measurement in spores was made by using the fluorescent Ca^{2+} indicator Fluo3-AM. The final concentration of Fluo3-AM was 10 μM prepared from a 5 mM Me_2SO stock solution. Final Me_2SO concentration was 0.2% or less, a concentration that had no discernible effect on spore viability. The buffer used was 10 mM Hepes, pH 7.4. Samples were observed with an Axiovert

200 Zeiss inverted microscope with a Mercury light source. Images were processed using Aquacosmos 2.5 software [28]. In some experiments either the Ca^{2+} chelator Bapta-AM, prepared from a 13 mM stock solution in Me_2SO, or 2 mM EGTA was used. Spores were preincubated with either Bapta-AM or EGTA for 30 min and then incubated with VTA_3 for different incubation times before the measurement of cytosolic Ca^{2+}.

Preparation of giant liposomes

Large unilamellar vesicles of asolectin (soybean lipids, type II-S; Sigma) or from mixtures of PtdCho/PtdEtn/PtdSer at 45 : 45 : 10 and 50 : 25 : 25 molar proportions were prepared at 25 mg·mL^{-1} in 10 mM Hepes (pH 7.5)/100 mM KCl and stored in liquid N_2 [29]. Giant liposomes (20–100 μm) were prepared by submitting asolectin vesicles to a cycle of partial dehydration/hydration, as reported previously [29].

Patch-clamp measurements

Asolectin giant liposomes (1–3 μL) were deposited on to 3.5-cm Petri dishes and mixed with 2 mL of a solution containing 10 mM KCl/10 mM Hepes (potassium salt), pH 7, for electrical recording (bath solution). Giga seals were formed on giant liposomes with microelectrodes of 7–10 MΩ resistance. Standard inside-out patch-clamp recordings [30] were performed using an Axopatch 200A (Axon Instruments, Union City, CA, USA), at a gain of 50 mV·pA^{-1}. Recordings were filtered at 1 kHz with an 8-pole Bessel filter (Frequency Devices, Haverhill, MA, USA). The holding potential was applied to the interior of the patch pipette, and the bath was maintained at virtual ground ($V = V_{bath} - V_{pipette}$). An Ag/AgCl wire was used as the reference electrode through an agar bridge. The data were analyzed with pClamp9 software (Axon Instruments). Patch electrodes were filled with a solution containing 100 mM KCl and 10 mM Hepes (potassium salt), pH 7 (pipette solution). After seal formation, VtA_3 was added to the bath solution at a concentration from 0.1 μM to 5 μM. VtA_3 was added with the pipette tip at a distance of 10–15 mm, with brief stirring. The recording was started immediately after addition. A pulse protocol (from +80 to −80 mV at 20-mV steps; 2 s of recording at each voltage) and/or a voltage ramp (from +80 to −80 mV during 3 s) were applied repetitively in these experiments. All measurements were made at room temperature.

Texas Red labelling of VtA_3

Conjugation of VtA_3 with Texas Red was performed in 20 mM Na_2HPO4 buffer, pH 7. Texas Red was dissolved in anhydrous dimethylformamide at a concentration of 100 mg·mL^{-1}, and an aliquot of 10 μL was immediately added to the protein solution (1 mg in 380 μL buffer) while stirring. The reaction mixture was incubated at 4 °C for 60 min. Conjugated protein was separated from unreacted dye by size-exclusion chromatography using Sephadex G-25. The degree of labelling was determined as the ratio of fluorophore to protein as previously described [31].

Permeabilization of spores

The Sytox® Green nucleic acid stain (Molecular Probes, Eugene, OR, USA) was used to evaluate the integrity of the plasma membrane of spore cells; Sytox® Green has already been used to demonstrate changes in membrane integrity induced on incubation with antimicrobial peptides [32]. Whereas it cannot cross the membrane of live cells, it readily penetrates disrupted plasma membranes before binding to nucleic acid, where it induces an intense fluorescence emission when excited under blue light illumination. Spores were incubated in 10 mM Hepes, pH 7.4 (control experiments) or exposed to 10 μM Texas Red-labelled VTA_3 for 5 min. After treatment, 10 μL of spore suspensions were mixed with a Sytox® Green solution (1 μM final concentration) and immediately viewed with an inverted confocal laser scanning microscope.

Confocal laser scanning microscopy

Fluorescence images were recorded using an inverted laser scanning microscope (Zeiss LSM5 Pascal) with a Plan-Apochromat 63×/1.4 oil-immersion objective and a HFT 488/543/633 dichroic mirror (Carl Zeiss Instruments, Zurich, Switzerland). A 488-nm Ar laser was used to excite the Sytox® Green (filtered with a 505 530-nm band pass), whereas a 543-nm He/Ne laser was used for excitation of Texas Red-labelled VtA_3 (filtered with a long pass filter < 560 nm). Optical sections of 1.8 μm through the centre of the spores or 4 μm for the liposomes were used for localization of the fluorescent signal. The protein concentration was 10 μM. When spores were visualized, nucleus localization was confirmed with Sytox® Green nuclear stain. Neither cells nor liposomes revealed autofluorescence.

Acknowledgements

This work was supported by grant BMC2002-00158 from MCYT, Spain (to J.V.). M.G. is a recipient of a predoctoral fellowship from CONICET, Argentina. The financial support of AECI, Spain, is gratefully acknowledged.

References

1 García-Olmedo F, Molina A, Alamillo JM & Rodríguez-Palenzuela. P (1998) Plant defense peptides. *Biopolymers* **47**, 479–491.

2 Florack DEA, Stiekema W & J (1994) Thionins: properties, possible biological roles and mechanisms of action. *Plant Mol Biol* **26**, 25–37.
3 Giudici M, Pascual R, de la Canal L, Pfüller K, Pfüller U & Villalaín J (2003) Interaction of viscotoxins A_3 and B with membrane model systems: implications to their mechanism of action. *Biophys J* **85**, 971–981.
4 Ochocka JR & Piotrowski A (2002) Biological active compounds from European mistletoe (*Viscum album* L.). *Can J Plant Pathol* **24**, 21–28.
5 Orrù S, Scaloni A, Giannattasio M, Urech K, Pucci P & Schaller G (1997) Amino acid sequence, S-S bridge arrangement and distribution in plant tissues of thionins from *Viscum album*. *Biol Chem* **378**, 986–996.
6 Schrader-Fischer G & Apel K (1993) cDNA-derived identification of novel thionin precursors in *Viscum album* that contain highly divergent thionin domains but conserved signal and acidic polypeptide domains. *Plant Mol Biol* **23**, 1233–1242.
7 Romagnoli S, Fogolari F, Catalano M, Zetta L, Schaller G, Urech K, Giannattasio M, Ragona L & Molinari H (2003) NMR solution structure of viscotoxin C1 from *Viscum album* species *Coloratum ohwi*: toward a structure-function analysis of viscotoxins. *Biochemistry* **42**, 12503–12510.
8 Ochocka JR & Piotrowski A (2002) Biological active compounds from European mistletoe (*Viscum album* L.). *Can J Plant Pathol* **24**, 21–28.
9 Büssing A, Stein GM, Wagner M, Wagner B, Schaller G, Pfüller U & Schietzel M (1999) Accidental cell death and generation of reactive oxygen intermediates in human lymphocytes induced by thionins from *Viscum album* L. *Eur J Biochem* **262**, 79–87.
10 Schaller G, Urech K & Giannattasio M (1996) Cytotoxicity of different viscotoxins and extracts from the European subspecies of *Viscum album* L. *Phytother Res* **10**, 473–477.
11 Romagnoli S, Ugolini R, Fogolari F, Schaller G, Urech K, Giannattasio M, Ragona L & Molinari H (2000) NMR structural determination of viscotoxin A3 from *Viscum album* L. *Biochem J* **350**, 569–577.
12 Carrasco L, Vázquez D, Hernández-Lucas C, Carbonero P & García-Olmedo F (1981) Thionins: plant peptides that modify membrane permeability in cultured mammalian cells. *Eur J Biochem* **116**, 185–189.
13 Holtorf S, Ludwig-Müller J, Apel K & Bohlemann H (1998) High-level expression of a viscotoxin in *Arabidopsis thaliana* gives enhanced resistance against *Plasmodiophora brassicae*. *Plant Mol Biol* **36**, 673–680.
14 Jung ML, Baudino S, Ribereau-Gayon G & Beck JP (1990) Characterization of cytotoxic proteins from mistletoe (*Viscum album* L.). *Cancer Lett* **51**, 103–108.
15 Tabiasco J, Pont F, Fournié J, J & Vercellone A (2002) Mistletoe viscotoxins increase natural killer cell-mediated cytotoxicity. *Eur J Biochem* **269**, 2591–2600.
16 Giudici AM, Regente MC, Villalaín J, Pfüller K, Pfüller U & De la Canal L (2004) Mistletoe viscotoxins induce membrane permeabilization and spore death in phytopathogenic fungi. *Physiol Plant* **121**, 2–7.
17 Stein GM, Schaller G, Pfüller U, Schiuetzel M & Büssing A (1999) Thionins from *Viscum album* L: influence of the viscotoxins on the activation of granulocytes. *Anticancer Res* **19**, 1037–1042.
18 Stein GM, Schaller G, Pfüller U, Wagner M, Wagner B, Schietzel M & Büssing A (1999) Characterisation of granulocyte stimulation by thionins from European mistletoe and from wheat. *Biochim Biophys Acta* **1426**, 80–90.
19 Edelhoch H (1967) Spectroscopic determination of tryptophan and tyrosine in proteins. *Biochemistry* **6**, 1948–1954.
20 Bligh EG & Dyer WJ (1959) A rapid method of total lipid extraction and purification. *Can J Biochem Physiol* **3**, 911–917.
21 Böttcher CSF & Fries C (1961) A rapid and sensitive sub-micro phosphorus determination. *Anal Chim Acta* **1061**, 297–303.
22 Lee DG, Park Y, Kim HN, Kim HK, Kim PI, Vhai BH & Hahm KS (2002) Antifungal mechanism of an antimicrobial peptide, HP (2–20), derived from N-terminus of *Helicobacter pylori* ribosomal protein L1 against *Candida albicans*. *Biochem Biophys Res Commun* **291**, 1006–1013.
23 Hope MJ, Bally MB, Webb G & Cullis PR (1985) Production of large unilamellar vesicles by a rapid extrusion procedure. Characterization of size distribution, trapped volume and ability to maintain a membrane potential. *Biochim Biophys Acta* **812**, 55–65.
24 Mishra VK, Palgunachari MN, Segrest JP & Anantharamaiah GM (1994) Interactions of synthetic peptide analogs of the class A amphipathic helix with lipids. Evidence for the snorkel hypothesis. *J Biol Chem* **269**, 7185–7191.
25 Krause KH, Fivaz. M, Monod A & van der Goot FG (1998) Aerolysin induces G-protein activation and Ca^{2+} release from intracellular stores in human granulocytes. *Biol Chem* **273**, 18122–18129.
26 Van der Heiden MG, Chandel NS, Williamson EK, Schumacker PT & Thompson CB (1997) Bcl-xL regulates the membrane potential and volume homeostasis of mitochondria. *Cell* **91**, 627–637.
27 Haugland RP (1996) *Handbook of Fluorescent Probes and Research Chemicals*, 6th edn. Molecular Probes, Inc, Eugene, OR.
28 Chandra S, Leinhos GM, Morrison GH & Hoch HC (1999) Imaging of total calcium in urediospore germlings of *Uromyces* by ion microscopy. *Fungal Genet Biol* **27**, 77–87.
29 Riquelme G, López E, García-Segura LM, Ferragut JA, González-Ros J & M (1990) Giant liposomes: a model

system in which to obtain patch-clamp recordings of ionic channels. *Biochemistry* **51**, 11215–11222.
30 Hamill OP, Marty A, Neher E, Sakmann B, Sigworth F & J (1981) Improved patch clamp technique for high-resolution current recording from cells and cell free patches. *Pfluegers Arch* **391**, 85–100.
31 Haugland RP (1995) Coupling of monoclonal antibodies with fluorophores. In *Methods in Molecular Biology: Monoclonal Antibody Protocols* (Davis WC, ed.), vol. 45, pp. 205–221. Humana Press, Totowa, NJ.
32 Rioux D, Jacobi V, Simard M & Hamelin RC (2000) Structural changes of spores of tree fungal pathogens after treatment with the designed antimicrobial peptide D2A21. *Can J Bot* **78**, 462–471.
33 Peberdy JF (1976) *Microbial and Plant Protoplasts*. Academic Press London, New York, San Francisco.
34 Barran LR & Miller RW (1976) Temperature-induced alterations in phospholipids of *Fusarium Oxysporum f sp Lycopersici*. *Can J Microbiol* **22**, 557–562.
35 Contreras LM, Aranda FJ, Gavilanes F, González-Ros José M & Villalaín J (2001) Structure and interaction with membrane model systems of a peptide derived from the major epitope region of HIV protein gp41: implications on viral fusion mechanism. *Biochemistry* **40**, 3196–3207.
36 Hughes P, Dennis E, Whitecross M, Llewellyn D & Gage P (2000) The cytotoxic plant protein,,-purothionin, forms ion channels in lipid membranes. *J Biol Chem* **275**, 823–827.
37 Llanos P, Henriquez M, Minic J, Elmorjani K, Marion D, Riquelme G, Molgo J & Benoit E (2004) Neuronal and muscular alterations caused by two wheat endosperm proteins, puroindoline-a and alpha1-purothionin, are due to ion pore formation. *Eur Biophys J* **33**, 283–284.
38 Green DR & Reed JC (1998) Mitochondria and apoptosis. *Science* **281**, 1309–1312.
39 Berridge MJ, Lipp P & Bootman MD (2000) The versatility and universality of calcium signalling. *Nat Rev Mol Cell Biol* **1**, 11–21.
40 Samuelsson G, Seger L & Olson T (1968) The amino acid sequence of viscotoxin A3 from European mistletoe (*Viscum album* L.). *Acta Chem Scand* **22**, 2624–2642.
41 Gullingsrud J & Schulten K (2004) Lipid bilayer pressure profiles and mechanosensitive channel gating. *Biophys J* **86**, 3496–3509.
42 Thevissen K, Ferket KK, Francois IE & Cammue BP (2003) Interactions of antifungal plant defensins with fungal membrane components. *Peptides* **24**, 1705–1712.
43 Martindale JL & Holbrook NJ (2002) Cellular response to oxidative stress: signaling for suicide and survival. *J Cell Physiol* **192**, 1–15.
44 Takeuchi K, Takahashi H, Sugai M, Iwai H, Kohno T, Sekimizu K, Natori S & Shimada I (2004) Channel-forming membrane permeabilization by an antibacterial protein, sapecin: determination of membrane-buried and oligomerization surfaces by NMR. *J Biol Chem* **279**, 4981–4987.
45 Debreczeni JE, Girmann B, Zeeck A, Kratzner R, Sheldrick G & M (2003) Structure of viscotoxin A_3: disulfide location from weak SAD data. *Acta Crystallogr D Biol Crystallogr* **59**, 2125–2132.
46 Teeter MM, Ma XQ, Rao U & Whitlow M (1990) Crystal structure of a protein-toxin α-1-purothionin at 2.5A and a comparison with predicted models. *Proteins* **8**, 118–132.
47 Takeuchi K, Takahashi H, Sugai M, Iwai H, Kohno T, Sekimizu K, Natori S & Shimada I (2004) Channel-forming membrane permeabilization by an antibacterial protein, sapecin: determination of membrane-buried and oligomerization surfaces by NMR. *J Biol Chem* **279**, 4981–4987.
48 Vernon LP & Rogers A (1992) Binding properties of *Pyrularia thionin* and *Naja naja kaouthia* cardiotoxin to human and animal erythrocytes and to murine P388 cells. *Toxicon* **30**, 711–721.
49 McIntosh TJ (2004) The 2004 Biophysical Society-Avanti Award in Lipids address: roles of bilayer structure and elastic properties in peptide localization in membranes. *Chem Phys Lipids* **130**, 83–98.
50 Caaveiro JM, Molina A, Rodriguez-Palenzuela P, Goñi FM & González-Mañas JM (1998) Interaction of wheat alpha-thionin with large unilamellar vesicles. *Protein Sci* **7**, 2567–2577.
51 Coulon A, Berkane E, Sautereau AM, Urech K, Rouge P & Lopez A (2002) Modes of membrane interaction of a natural cysteine-rich peptide: viscotoxin A_3. *Biochim Biophys Acta* **1559**, 145–159.
52 Murray D, Hermida-Matsumoto L, Buser CA, Tsang J, Sigal CT, Ben-Tal N, Honig B, Resh MD & McLaughlin S (1998) Electrostatics and the membrane association of Src: theory and experiment. *Biochemistry* **37**, 2145–2159.